doi:10.14311/ppt.2025.3.190
Plasma Physics and Technology **12**(3):190–196, 2025

NUMERICAL MODELING OF ELECTRIC ARC IN A LOW VOLTAGE BREAKING CHAMBER

A. Gatri[a, b, *], J-J. Gonzalez[a], P. Freton[a], P. Joyeux[b], F. Sambou[a]

[a] *LAPLACE, UMR 5213 CNRS-UPS-INP, Université Paul Sabatier, 118 rte de Narbonne, bat3R3, 31062 Toulouse Cedex, France*

[b] *Hager Group, Obernai 132 Bd de l'Europe, France*

[*] arsalen.gatri@laplace.univ-tlse.fr

Abstract. This work presents the development of a MagnetoHydroDynamic (MHD) model to simulate electric arc behavior in a low-voltage circuit breaker chamber. The modeling process began with a simplified geometry to validate key phenomena such as arc displacement, segmentation, and voltage rise, showing good agreement with literature. To approach realistic conditions, contact rotation was implemented using a layering technique, improving numerical accuracy and avoiding mesh deformation. A current-limiting mechanism and electrical network coupling were also introduced, enabling dynamic current input. These modules were integrated into a 3D geometry representing a real chamber, successfully reproducing arc evolution under realistic conditions. The model captures complex arc physics and helps in future design optimization of low-voltage devices.

Keywords: Low-voltage circuit breaker, arc modeling, air plasma, simulation.

1. Introduction

Low-voltage circuit breakers (LVCBs) are essential components in both industrial and residential electrical systems, ensuring the protection of users and installations. Their critical function has motivated many research studies dedicated to improving their performance and reliability. In these devices, current interruption is achieved primarily through current-limiting mechanisms. When a current fault occurs, the contacts open and an electric arc is initiated. The design of the LVCB facilitates the movement of the arc into the breaking chamber, driven by pressure forces and the Lorentz force resulting from the current flow in the arc runners.

Inside the breaking chamber, the arc is segmented into multiple sub-arcs by metallic splitters. This segmentation leads to an increased arc voltage due to additional cathode and anode voltage drops, which helps to force the current toward zero and achieve successful interruption. To optimize the breaking capacity and improve the operational reliability of the breaker, it is crucial to understand the physical behavior of the arc throughout its evolution, from initiation and movement to quenching and extinction.

Experimental studies have traditionally investigated physical quantities such as arc velocity, arc root positioning, and contact separation speed, using high-speed imaging techniques [1–3]. In parallel, numerical simulations have enabled detailed analysis of arc dynamics in increasingly complex geometrical configurations [4–6]. However, the physical processes occurring at the plasma-electrode interface are particularly intricate and remain difficult to resolve in a global plasma flow description. Recent studies [4, 7, 8] have introduced macroscopic modeling approaches to represent these interactions, incorporating additional resistivity at the electrode-plasma interface. This allows for a more accurate estimation of the arc voltage, particularly in the presence of arc splitters.

Building on this foundation, the present work introduces a magnetohydrodynamic (MHD) model to simulate the behavior of an electric arc in a low-voltage circuit breaker. The model begins with a simplified reference geometry that validates key arc phenomena such as displacement, segmentation, and voltage evolution, with results consistent with the existing literature. To approach realistic operating conditions, the model incorporates several advanced physical mechanisms such as voltage drop due to segmentation of the arc between splitter plates, contact rotation, and a current limiting mechanism by coupling the model with the external network equations. In contrast to previous studies, which generally address these physical mechanisms separately, the present work proposes a model that integrates all of these modules into a unified environment. A new technique for contact opening is also proposed that helps reduce computational time and improve numerical stability.

In this paper, geometries, equations, hypotheses, and developed modules are presented in Section 2. The results obtained are discussed in Section 3. Lastly, a conclusion is given in Section 4.

2. Numerical model

This section presents the main characteristics of the model. Section 2.1 describes the governing fluid dynamics equations, while Section 2.2 introduces the electromagnetic equations. The assumptions of the model are outlined in Section 2.3. Section 2.4 discusses the implementation of the additional resistivity approach. The geometric configuration and mesh are detailed in Section 2.5. Section 2.6 highlights the model upgrades and newly developed modules. Finally, the results obtained in a real breaking chamber are presented in Section 3.

2.1. Fluid equations

A three-dimensional hydrodynamic model is employed using Ansys Fluent [9] to simulate the behavior of the air plasma, solving both the dynamics of the gas flow and the transport of energy. To take into account the electromagnetic phenomena associated with the arc, the model is coupled with Maxwell's equations. The coupling is achieved by introducing custom functions and additional scalar fields, which enable the simulation of current distribution and the self-induced magnetic field generated by the arc [7].

The electric arc in a LVCB is modeled as a conductive fluid using the Navier–Stokes equations. To account for the arc's conductive and thermal effects, additional source terms are added to the governing equations. Specifically, the momentum equations include Lorentz force contributions, while the energy equation is extended to account for Joule heating, radiative heat losses, and electron enthalpy transport.

□ Mass conservation equation

$$\frac{\partial \rho}{\partial t} + \vec{\nabla} \cdot (\rho \vec{v}) = 0 \tag{1}$$

□ Momentum conservation equation

$$\frac{\partial(\rho \vec{v})}{\partial t} + \vec{\nabla} \cdot (\rho \vec{v} \cdot \vec{v}) = \vec{\nabla} \cdot (\eta \vec{\nabla} \vec{v}) - \vec{\nabla} p + (\vec{j} \times \vec{B}) + s_\nu \tag{2}$$

□ Energy conservation equation

$$\frac{\partial(\rho H)}{\partial t} + \vec{\nabla} \cdot (\rho H \vec{v}) = \frac{\partial p}{\partial t} + \vec{\nabla} \cdot \left(\frac{\lambda}{c_p} \vec{\nabla} H \right) + \sigma \vec{E}^2 - q_{\text{rad}} + S_h \tag{3}$$

$\vec{v}$ is the velocity vector, p the pressure, H the enthalpy, $\vec{j}$ the current density vector, $\vec{B}$ the magnetic field, ρ is the mass density, η the dynamic viscosity, λ the thermal conductivity, C_p the specific heat, σ the electrical conductivity, q_{rad}=$4\pi\epsilon_N$, ϵ_N is the net emission coefficient calculated for a radius $R_p = 5\,\text{mm}$, S_ν contains supplementary terms of viscous tensors, S_h is an additional source term that is required to take into account the enthalpy flux of electrons [10].

2.2. Electromagnetic equations

The electromagnetic process is governed by Maxwell's equations, which is another complex system of differential equations [11][12]. The magnetic field and the electric potential are calculated in the whole domain. The scalar potential and the vector potential equations are used to calculate the electromagnetic fields:

$$\vec{B} = \vec{\nabla} \times \vec{A} \tag{4}$$

$$\vec{E} = -\vec{\nabla} V - \frac{\partial \vec{A}}{\partial t} \tag{5}$$

$$\vec{j} = \sigma \vec{E} \tag{6}$$

$$\vec{\nabla} \cdot (\vec{\nabla} \vec{A}) = -\mu \vec{j} \tag{7}$$

$$\vec{\nabla} \cdot (\sigma \vec{\nabla} V) = 0 \tag{8}$$

In the equations above, $\vec{A}$ is the vector potential, V is the electric potential, and μ is the air magnetic permeability. Since the temporal variations of the electromagnetic fields are slow, inductive effects are negligible, and the system can be treated in a quasi-static regime. This assumption justifies neglecting the $\frac{\partial \vec{A}}{\partial t}$ term in Equation (5).

To close the system for the magnetic field calculation, the Biot&Savart formulation is used at the edges of the domain as a Dirichlet boundary condition. The equation is formulated as follows [12]:

$$\vec{A} = \frac{\mu}{4\pi} \iiint_{\text{volume}} \frac{\vec{J}(\vec{r'})}{|\vec{r} - \vec{r'}|} \, dV \tag{9}$$

This equation is used to calculate the magnetic field $\vec{B}$ resulting at position r and distanced of r' from the electrical current in a domain of volume V. The resolution of the equation (9) is time consuming, however, in our case, we use a hybrid formulation which means that the magnetic field within the plasma domain is calculated using the vector potential equations to determine the self-induced magnetic field and the Biot&Savart formulation is only used as a boundary condition [12].

2.3. Hypotheses

The following assumptions have been used :

□ The air medium plasma is assumed to be in Local Thermodynamic Equilibrium (LTE). So, only one energy equation is solved for the fluid, assuming all the species have the same temperature. This assumption is also used to calculate the plasma composition (evolution of the species densities), the transport and thermodynamic properties [13];

□ The flow is considered laminar. The Reynolds number is assumed to be small due to the high viscosity of the arc and many research which have been performed on a simplified arc chamber show the validity of this assumption [14][15];

□ Arc ignition is not described, and the calculation begins with an initial arbitrary temperature channel equal to 20000 K;

□ Vapours coming from the walls and the erosion of the electrodes are not taken into account. So, copper vapours from the runners, iron vapours from the splitters or PA66 ($C_6H_{11}O_1N_1$) from lateral walls are not considered even if they may change the plasma properties and the arc motion [2, 16–18];

- Radiation is treated using the net emission coefficient method [19]. Other methods can be adopted for the radiation as the P1 model or the DOM using mean absorption coefficients. These methods allow not only to consider the losses due to the emission of the hottest regions, but also to consider the absorption of the radiation in the surrounding plasma [20]. Certainly, the choice of the radiation model directly affects the plasma properties and so the arc motion prediction. Nevertheless, in this paper, we focus our study on the general behavior of the arc;
- Splitters are not treated as ferromagnetic materials.

2.4. Additional resistivity model

Anode and cathode sheaths are non-equilibrium zones near the electrode surfaces. In these zones, the physics is complex and difficult to couple with the LTE plasma. Then, to allow the passage of the current from the solid material to the plasma, a simplified electrical approach is adopted using an additional localized electrical conductivity σ_{eff} within these zones, defined by:

$$\sigma_{\text{eff}} = J\frac{\Delta y}{U_s} \tag{10}$$

Where U_s is the additional voltage drop, J is the current density, and $\Delta y = 0.1\,\text{mm}$ is the thickness of the sheath layer. This size is predefined for the anodic and cathodic sheath regions in the Lowke model [21] and is generally used in the literature [22, 23]. Then the mesh size in the region near the electrode is equal to 0.1 mm.

The effective conductivity σ_{eff} is strongly influenced by the nature of the plasma gas, the electrode materials, and the surface conditions. Equation (10) allows to determine an effective conductivity close to the electrode wall. It is governed by the U-J curves determined from the studies [23–25], which presented different curves (a, b, c, d) with different peak values determined experimentally for different configurations and varied materials.

Before the formation of a new arc root, an ignition voltage that corresponds to the peaks should be exceeded at low current densities [23]. The existence of ignition voltage before the formation of the arc root was observed in measurements [5][26]. For higher current densities, that is, when the current flows entirely through the arc root, the voltage drop becomes constant and independent of the current density. For a copper cathode, this voltage drop is roughly approximated by U_s=10 V, as reported in [27–29].

For this work, we have chosen curve (c) [30]. It represents a voltage hump (ignition voltage) before the arc root formation of $U_0 = 17.2\,\text{V}$, which corresponds to the experimental value for the copper material.

The total arc voltage increases with the number of sheath voltages. Taking into account the voltage drop in these sheath layers helps improve the physical understanding of arc root movement and provides a more accurate representation of the total arc voltage.

2.5. Simplified geometry

Figure 1 shows a simplified geometry of the arc-breaking chamber. This initial configuration allowed the validation of essential physics of the electric arc in low-voltage breaking chamber, such as arc displacement, influence of electromagnetic and pressure forces, and segmentation by studying the influence of the number of splitter plates on the arc voltage rise. The numerical results obtained from this model showed good agreement with the literature, as the general arc behavior and the additional voltage of 20 V match numerical and experimental results reported in [7, 31–33]. This provides a solid foundation for the future integration of additional physical details and more complex geometries, ultimately aiming to replicate the full behavior of low-voltage circuit breakers in real circuit conditions.

The geometry was meshed using ANSYS ICEM CFD. A structured hexahedral mesh was selected to ensure high accuracy and better alignment with the flow and field gradients. The entire domain was discretized with a uniform cell size of $0.1\,\text{mm}^3$, providing sufficient resolution to capture the detailed behavior of the arc.

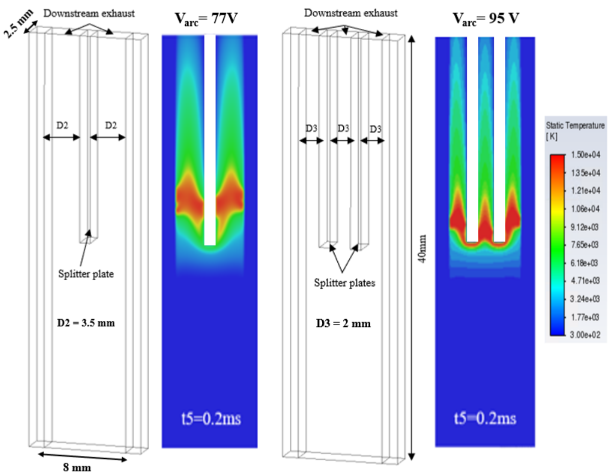

Figure 1. Simplified arc breaking geometry with different number of splitter plates.

2.6. Model upgrade

Building upon the simplified geometry, the methodology was extended to incorporate more realistic features of the LVCB. This upgraded model includes the addition of a rotating contact, represented through the layering technique, which enables an accurate simulation of mechanical movement during arc initiation. Unlike the initial model, which used a constant current or an experimental current curve as input, the new approach integrates the arc simulation with an external electrical network. This network coupling allows the current to dynamically respond to the arc's behavior and circuit conditions, providing a more realistic representation of the arc breaking via its fundamental principle: Current limiting. In Figure 2, we present the main characteristics of the model to be taken into account in a real arc breaking chamber.

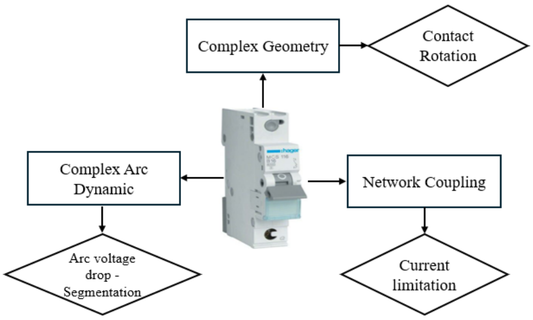

Figure 2. Main real arc breaking chamber model characteristics

2.6.1. Network coupling

Current-limiting behavior, achieved by increasing the arc voltage using splitter plates, is a key aspect of low-voltage breaking. By incorporating this into the model, we can more accurately represent the voltage increase and current decrease during arc extinction. For that, we need to couple our model with the external circuit, presented in Figure 3. This allows for dynamic interaction between the arc and the electrical circuit, capturing the transient current behavior.

Our experimental setup, designed to study the movement of the arc in a breaking chamber, is connected to a capacitor bench. This bench allows us to vary the current intensity while maintaining the same AC frequency, depending on the charging voltage and the (L, C) couple values.

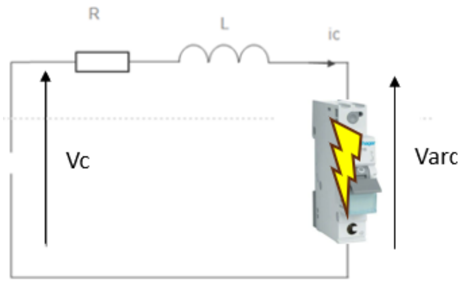

Figure 3. Experimental setup - RLC circuit

Based on this experimental configuration, we can define the differential equation (11) that governs the circuit in the presence of an electric arc.

$$V_c = V_{arc} + V_R + V_L \tag{11}$$

The nonlinear differential equation (11) is discretized and solved iteratively using the Euler method as mentioned in Figure 4. The solution of the differential equation is fully developed in a User-Defined Function (UDF) in Fluent. The results of this module can be found in [34].

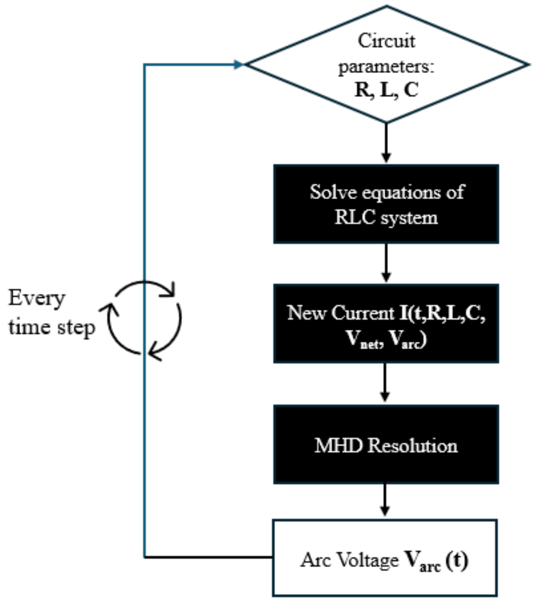

Figure 4. Network coupling iterative process

2.6.2. Contact rotation

Reproducing the motion of the moving contact during the opening process in low-voltage arc chambers poses both physical and computational challenges. Conventional methods, such as rigid body translation of contact [35–38] or dynamic remeshing [39–41], are typically limited by geometric flexibility, higher numerical instability, and large computational cost.

To address these limitations, a numerical modeling approach has been adopted using the layering technique, as presented in Figure 5. This method allows to create a structured mesh with multiple layers of cells to accurately capture rapid changes in flow properties while maintaining the same number of cells. In this structure, cells of 0.1 mm are progressively introduced on one side of the domain and removed on the opposite side, following rotation of contact. This significantly reduces computational time while enhancing the precision of the solution in critical arc zones. It also enhances numerical stability and provides precise control over the opening process.

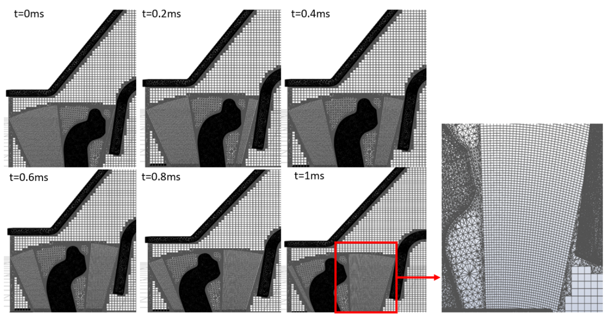

Figure 5. Opening process of moving contact

2.6.3. Complex geometry

The geometrical configuration used in this study, illustrated in Figure 6, is derived from a real industrial breaking chamber and retains its essential structural complexity. This realistic geometry includes critical features that influence arc behavior, such as rotating contact, arc runners, and real-form splitters. To reduce the calculation time, certain regions, specifically the volume behind the contact system and the venting area at the outlet, were excluded from the simulation domain. Despite these simplifications, the model preserves the core physical characteristics necessary to accurately capture arc dynamics. The primary objective at this stage is to establish a robust and representative model capable of reproducing realistic arc phenomena within the breaking chamber. This also serves to evaluate the performance of the developed simulation modules in capturing key physical processes, thereby validating their reliability for future parametric studies and design optimizations.

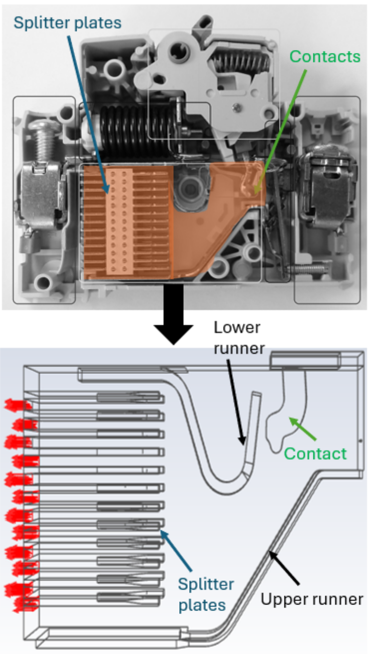

Figure 6. LVCB real breaking chamber

3. Simulation results

This section presents the results obtained from the proposed model. The current intensity varies over time and is determined based on the circuit parameters, reaching values up to 1.5 kA. Figure 7 illustrates the computed temperature distribution during the evolution of the arc within the breaking chamber, highlighting the key phases of the arc behavior :
1) arc elongation between the contacts; 2) arc commutation from the contacts to the arc runner; 3) arc displacement between the runners; 4) arc splitting process; 5) arc re-striking (back commutation).

The initial stage involving arc ignition and the onset of contact separation is not included in the simulation. Instead, the model begins at a relative time of $t_R = t_{real} + 0.5\,\text{ms}$, corresponding to a current of $I = 1300\,\text{A}$.

Initially, the arc forms and elongates between the contacts, driven by magnetic forces. As it extends, the hot plasma begins to interact with the upper and lower runners. At $t_R = 0.3\,\text{ms}$, the arc is fully commuted from the moving contact to the upper arc runner. Then it continues its displacement toward the splitter region, driven by both electromagnetic and pressure forces in the chamber. By $t_R = 0.5\,\text{ms}$, the arc root establishes contact with the splitter plates, initiating the splitting process. Then, the arc column is progressively divided into multiple sub-arcs between the splitters, and the arc voltage rises to approximately $\approx 210\,\text{V}$. However, at $t_R = 0.7\,\text{ms}$, a new arc root unexpectedly forms on the lower runner behind the main arc column. This results in the creation of a secondary current path, effectively replacing the previous one. This phenomenon is referred to as restrike or back-commutation. As a consequence, the segmentation process must restart from this new arc root, and the arc voltage falls to approximately ≈ 187 V. This can be detrimental to the breaking process, as it delays current interruption and increases energy dissipation in the device. Finally, the arc is divided once again between the splitters, and a total voltage of 310 V is reached.

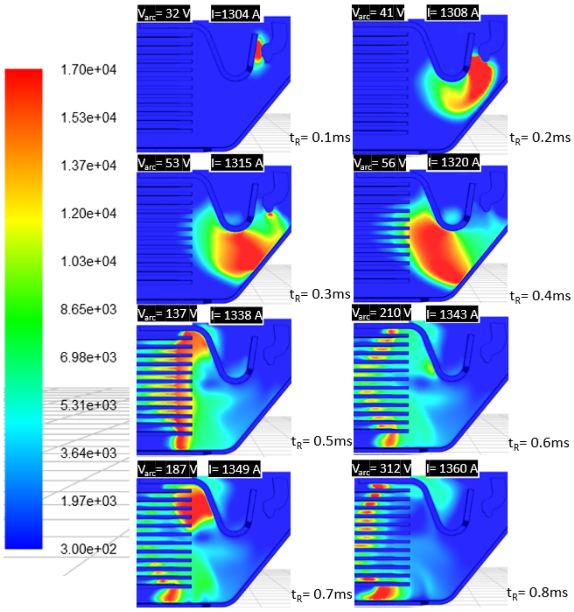

Figure 7. Arc temperature distribution in the breaking chamber, and corresponding values of V and I.

Although the venting regions are simplified, this simulation shows the ability of the model to capture and visualize the transient evolution of the arc in realistic circuit breaker geometry. Such results offer a valuable tool for understanding the arc behavior and serve as a solid foundation for future studies aimed at optimizing design and improving device performance.

4. Conclusion

This study has demonstrated the successful development and implementation of an advanced MHD model to simulate the behavior of an electric arc in a low-voltage circuit breaker. Starting from a simplified configuration, the model was progressively enhanced by incorporating key physical and computational features. An additional resistivity approach was introduced to more accurately represent voltage drops near the electrodes. The simulation was extended to handle a complex 3D geometry closely resembling a real breaking chamber. A novel layering technique was implemented to model rotating contact with variable speed, allowing an accurate representation of contact opening and reducing computational time while improving the precision of the solution in critical zones. Furthermore, the arc model was coupled to an external electrical network, ensuring realistic operating conditions. These advancements significantly enhance the model's predictive capability, deepen the understanding of arc dynamics in switching devices, and provide a solid foundation for future research focused on optimizing circuit breaker design and performance.

References

[1] J Quéméneur. *Etude des forces à l'origine du déplacement d'un arc électrique dans un disjoncteur basse-tension*. PhD thesis, 2016. Publication Title: Thèse.

[2] X. Li, D. Chen, R. Dai, and Y. Geng. Study of the influence of arc ignition position on arc motion in low-voltage circuit breaker. *IEEE Transactions on Plasma Science*, 35(2 III):491–497, April 2007. doi:10.1109/TPS.2007.892579.

[3] J. Lu, J.-J. Gonzalez, P. Freton, et al. Experimental Studies of Arc Motion Between Two Parallel Runners with Splitter Plates. *Plasma Physics and Technology*, 7(1):16–20, June 2020. doi:10.14311/ppt.2020.1.16.

[4] Mingzhe Rong, Yi Wu, Fei Yang, et al. Numerical research on switching arc of circuit breaker. In *2011 1st International Conference on Electric Power Equipment - Switching Technology*, pages 488–491, Xi'an, China, October 2011. IEEE. ISBN 978-1-4577-1272-2 978-1-4577-1273-9 978-1-4577-1271-5. URL: http://ieeexplore.ieee.org/document/6123036/, doi:10.1109/ICEPE-ST.2011.6123036.

[5] M. Lindmayer, E. Marzahn, A. Mutzke, et al. The process of arc splitting between metal plates in low voltage arc chutes. *IEEE Transactions on Components and Packaging Technologies*, 29(2):310–317, June 2006. doi:10.1109/TCAPT.2006.875902.

[6] A. Mutzke, T. Rüther, M. Lindmayer, and M. Kurrat. Arc behavior in low-voltage arc chambers. *EPJ Applied Physics*, 49(2), January 2010. doi:10.1051/epjap/2010001.

[7] Jingjing Lu. *Caractérisation du comportement du plasma dans un disjoncteur basse tension par le développement d'un outil numérique et d'expériences associées*. PhD thesis, 2020. Publication Title: Thèse.

[8] J. Yin, Q. Wang, and X. Li. Simulation analysis of arc evolution process in multiple parallel contact systems. *IEEE Transactions on Plasma Science*, 46(8):2788–2793, 2018. doi:10.1109/TPS.2018.2828330.

[9] ANSYS. Ansys Fluent Customization Manual. Technical report, 2021. URL: http://www.ansys.com.

[10] Maëva COURREGE. *Caractérisation des interactions plasma/parois dans un disjoncteur haute tension*. PhD thesis, 2017.

[11] F. Karetta and M. Lindmayer. Simulation of the gasdynamic and electromagnetic processes in low voltage switching arcs. *IEEE*, 1996.

[12] P. Freton, J. J. Gonzalez, M. Masquère, and F. Reichert. Magnetic field approaches in dc thermal plasma modelling. *Journal of Physics D: Applied Physics*, 44(34), August 2011. doi:10.1088/0022-3727/44/34/345202.

[13] Vacquié Serge. *L'arc électrique*. 2000.

[14] F. Yang, M. Rong, Y. Wu, et al. Numerical analysis of the influence of splitter-plate erosion on an air arc in the quenching chamber of a low-voltage circuit breaker. *Journal of Physics D: Applied Physics*, 43(43), November 2010. doi:10.1088/0022-3727/43/43/434011.

[15] A. Gleizes, J. J. Gonzalez, and P. Freton. Thermal plasma modelling. *Journal of Physics D: Applied Physics*, 38(9), May 2005. doi:10.1088/0022-3727/38/9/R01.

[16] L. Xingwen, C. E. Degui Li Zhipeng, and W. Qian. Simulation of the Effects of Several Factors on Arc Plasma Behavior in Low Voltage Circuit Breaker Simulation of the Effects of Several Factors on Arc Plasma Behavior in Low Voltage Circuit Breaker*. Technical report, 2005. Publication Title: Plasma Science and Technology Plasma Science & Technology Issue: 5 ISBN: 130.120.97.16.

[17] M. Rong, Y. Wu, Q. Yang, et al. Simulation on arc movement under effects of quenching chamber configuration and magnetic field for low-voltage circuit breaker. *IEICE transactions on electronics*, 88(8):1577–1583, 2005. Publisher: The Institute of Electronics, Information and Communication Engineers.

[18] Y. Qian, R. Mingzhe, A. B. Murphy, and W. Yi. The influence of medium on low-voltage circuit breaker arcs. *Plasma Science and Technology*, 8(6):680, 2006. Publisher: IOP Publishing.

[19] Y. Naghizadeh-Kashani, Y. Cressault, and A. Gleizes. Net emission coefficient of air thermal plasmas. Technical report, 2002. Publication Title: J. Phys. D: Appl. Phys Volume: 35.

[20] F. Reichert, J. J. Gonzalez, and P. Freton. Modelling and simulation of radiative energy transfer in high-voltage circuit breakers. *Journal of Physics D: Applied Physics*, 45(37), September 2012. doi:10.1088/0022-3727/45/37/375201.

[21] J. J. Lowke and M. Tanaka. 'LTE-diffusion approximation' for arc calculations. *Journal of Physics D: Applied Physics*, 39(16):3634–3643, August 2006. doi:10.1088/0022-3727/39/16/017.

[22] M. S. Benilovt and A. Marottaf. A model of the cathode region of atmospheric pressure arcs. Technical report, 1995. Publication Title: J. Phys. D: Appl. Phys Volume: 28. URL: http://iopscience.iop.org/0022-3727/28/9/015.

[23] Z. Sun, M. Rong, F. Yang, et al. Numerical modeling of arc splitting process with ferromagnetic plate. *IEEE Transactions on Plasma Science*, 36(4 PART 1):1072–1073, August 2008. doi:10.1109/TPS.2004.924559.

[24] F. Yang, M. Rong, Y. Wu, et al. Numerical analysis of arc characteristics of splitting process considering ferromagnetic plate in low-voltage arc chamber. *IEEE Transactions on Plasma Science*, 38(11 PART 2):3219–3225, November 2010. doi:10.1109/TPS.2010.2070084.

[25] M. Rong, F. Yang, Y. Wu, et al. Simulation of arc characteristics in miniature circuit breaker. *IEEE Transactions on Plasma Science*, 38(9 PART 1):2306–2311, September 2010. doi:10.1109/TPS.2010.2050703.

[26] T. Rüther, A. Mutzke, M. Lindmayer, and M. Kurrat. The formation of arc roots on a metallic splitter plate in low-voltage arc chambers. In *23rd International Conference on Electrical Contacts, ICEC 2006 - together with the 6th International Session on Electromechanical Devices, IS-EMD 2006*, 2006.

[27] A. Erk and M. Schmelzle. *Grundlagen der Schaltgerätetechnik: Kontaktglieder und Löscheinrichtungen elektrischer Schaltgeräte der Energietechnik*. Springer, 1974.

[28] G. Hertz and R. Rompe. *Einführung in die Plasmaphysik und ihre technische Anwendung*. Walter de Gruyter GmbH & Co KG, 1968.

[29] M. Lindmayer, E. Vinaricky, F. Berger, et al. Schaltgeräte, elektromechanische bauelemente und sicherungen. In *Elektrische Kontakte, Werkstoffe und Anwendungen: Grundlagen, Technologien, Prüfverfahren*, pages 603–814. Springer, 2016.

[30] A. Mutzke, T. Rtither, M. Kurrat, et al. Modeling the Arc Splitting Process in Low-Voltage Arc Chutes. *Electrical Contacts - 2007 Proceedings of the 53rd IEEE Holm Conference on Electrical Contacts*, 2007.

[31] J. Quéméneur, J. Lu, J.-J. Gonzalez, et al. Arc motion in low voltage circuit breaker (LVCB) experimental and theoretical approaches. 8(2):35–45, 2019. doi:10.5923/j.scit.20180802.02.

[32] A. Iturregi, B. Barbu, E. Torres, et al. Electric Arc in Low-Voltage Circuit Breakers: Experiments and Simulation. *IEEE Transactions on Plasma Science*, 45(1):113–120, January 2017. Publisher: Institute of Electrical and Electronics Engineers Inc. doi:10.1109/TPS.2016.2633400.

[33] A. Iturregi Aio. Modelization and analysis of the electric arc in low voltage circuit breakers. 2013.

[34] A. Gatri, J.-J. Gonzalez, P. Freton, and P. Joyeux. Limitation de courant dans une chambre de coupure à basse tension. *Journal International de Technologie, de l'Innovation, de la Physique, de l'Energie et de l'Environnement*, 9(1), 2025.

[35] Y. Liu, D. Chen, H. Yuan, et al. Research of dynamic optimization for the cam design structure of MCCB. *IEEE Transactions on Components, Packaging and Manufacturing Technology*, 6(3):390–399, 2016.

[36] D. Shin, J. W. McBride, and I. O. Golosnoy. Arc modeling to predict arc extinction in low-voltage switching devices. In *2018 IEEE Holm Conference on Electrical Contacts*, pages 222–228. IEEE, 2018.

[37] F. Yang, R. Ma, Y. Wu, et al. Numerical study on Arc plasma behavior during Arc commutation process in direct current circuit breaker. *Plasma Science and Technology*, 14(2):167–171, February 2012. doi:10.1088/1009-0630/14/2/16.

[38] J. Almurr, W. Bussière, J. Hertzog, and D. Rochette. Numerical investigations on the electric arc behavior upon contact opening in a low-voltage switch under the effect of external magnetic field. *Electric Power Systems Research*, 209:107945, 2022. doi:10.1016/j.epsr.2022.107945.

[39] M. Rong, Q. Ma, Y. Wu, et al. The influence of electrode erosion on the air arc in a low-voltage circuit breaker. *Journal of Applied Physics*, 106(2), 2009. doi:10.1063/1.3176983.

[40] Y. Wu, M. Rong, Z. Sun, et al. Numerical analysis of arc plasma behaviour during contact opening process in low-voltage switching device. *Journal of Physics D: Applied Physics*, 40(3):795, 2007. doi:10.1088/0022-3727/40/3/016.

[41] Y. Wu, M. Rong, F. Yang, et al. Numerical modeling of arc root transfer during contact opening in a low-voltage air circuit breaker. *IEEE transactions on plasma science*, 36(4):1074–1075, 2008. doi:10.1109/TPS.2008.924634.